Schizophrenia Bulletin Open
https://doi.org/10.1093/schizbullopen/sgae002

Aberrant Brain Dynamics in Individuals With Clinical High Risk of Psychosis

Jochen Kindler[1,7], Takuya Ishida[2,7], Chantal Michel[1,*], Arndt-Lukas Klaassen[1], Miriam Stüble[1,3], Nadja Zimmermann[1,3,4], Roland Wiest[5], Michael Kaess[1,6], and Yosuke Morishima[*,4,*]

[1]University Hospital of Child and Adolescent Psychiatry and Psychotherapy, University of Bern, Bern, Switzerland; [2]Department of Neuropsychiatry, Graduate School of Wakayama Medical University, Kimiidera, Japan; [3]Graduate School for Health Sciences, University of Bern, Bern, Switzerland; [4]Translational Research Center, University Hospital of Psychiatry and Psychotherapy, University of Bern, Bern, Switzerland; [5]University Institute of Diagnostic and Interventional Neuroradiology, Inselspital, University of Bern, Bern, Switzerland; [6]Department of Child and Adolescent Psychiatry, Center for Psychosocial Medicine, University Hospital Heidelberg, Heidelberg, Germany

[7]Equally contributing first authors.

[*]To whom correspondence should be addressed; Translational Research Center, University Hospital of Psychiatry and Psychotherapy, University of Bern, Bolligenstrasse 111, 3000 Bern, Switzerland; Tel: +41-31-932-8705; Fax: +41-31-932-9961; e-mail: yosuke.morishima@unibe.ch

***Background*: Resting-state network (RSN) functional connectivity analyses have profoundly influenced our understanding of the pathophysiology of psychoses and their clinical high risk (CHR) states. However, conventional RSN analyses address the static nature of large-scale brain networks. In contrast, novel methodological approaches aim to assess the momentum state and temporal dynamics of brain network interactions.*Methods*: Fifty CHR individuals and 33 healthy controls (HC) completed a resting-state functional MRI scan. We performed an Energy Landscape analysis, a data-driven method using the pairwise maximum entropy model (MEM), to describe large-scale brain network dynamics such as duration and frequency of, and transition between, different brain states. We compared those measures between CHR and HC, and examined the association between neuropsychological measures and neural dynamics in CHR.*Results*: Our main finding is a significantly increased duration, frequency, and higher transition rates to an infrequent brain state with coactivation of the salience, limbic, default mode, and somatomotor RSNs in CHR as compared to HC. Transition of brain dynamics from this brain state was significantly correlated with processing speed in CHR.*Conclusion*: In CHR, temporal brain dynamics are attracted to an infrequent brain state, reflecting more frequent and longer occurrence of aberrant interactions of default mode, salience, and limbic networks. Concurrently, more frequent and longer occurrence of the brain state is associated with core cognitive dysfunctions, predictors of future onset of full-blown psychosis.**

Key words: dynamic functional connectivity/psychosis/cognitive dysfunction/network/energy landscape/prodromal state

Introduction

Despite low prevalence rates, psychoses are amongst the highest causes for disability-adjusted life years due to their manifestation early in life and generally low remission rates.[1] First-episode psychotic disorders are often preceded by a prodromal phase characterized by a range of symptoms related to clinical high risk (CHR), as well as other mental health problems and psychosocial deficits. During this phase, individuals may seek help.[2,3] The prodromal phase provides a promising starting point for indicated prevention efforts that aim to reduce CHR symptoms and prevent the progression to frank psychosis.[4] Within 1 year, about 15% of CHR patients will convert to psychosis, whereas another 10% will convert within the following 2 years.[5] Even though the majority of CHR patients do not go on to develop psychosis, neurobiological data on brain functions suggest that many findings in psychosis can be traced back to CHR states, though with lower effect sizes.[6,7] Thus, the CHR status may offer a window into the pathophysiology of psychosis, with fewer confounders than those that may be more evident in fully-manifest psychosis (and therefore, potentially a more reliable point of measuring symptoms), such as physical disorders, lifestyle differences, nicotine abuse, age effects, or medication status. From a neurobiological perspective, the disconnection hypothesis of psychosis[8]

suggests a failure of functional integration in distributed neuronal systems that heavily depend on abnormal synaptic transmission. At a system level, abnormal synaptic transmission may cause aberrant, eg, increased or decreased, interactions among brain networks. The aberrant interactions result in maladaptive cognitive processes and failures in predictive coding, leading to aberrant salience and giving rise to positive psychotic symptoms.

Resting-state fMRI (magnetic resonance imaging) provides a measure of brain activity at rest and allows for the addressing of the states of large-scale brain networks. Research on resting-state fMRI networks has revealed functionally integrated clusters of brain areas, such as the default mode network (DMN) related to internally oriented attention, and deactivated during task performance; the frontoparietal network (FPN) involved in top-down regulation of various cognitive operations; the dorsal attention network (DAN) important for guiding attention; the salience network (SAN) involved in monitoring relevance of events; the visual network (VIN) involved in visual processing; the limbic network (LIN) responsible for emotion regulation and memory performance; and the somatomotor network (SMN) relevant for coordination and integration of motor activity.[9] Many studies have investigated resting-state connectivity in psychosis and found reduced connectivity in most of these networks, but also increased connectivity in the SAN and DMN, eg.[10,11] According to the disconnection hypothesis, these primarily functional aberrations are caused by genetic alterations[12] and, more importantly, would already be evident before the onset of fully-manifest psychosis, such as in CHR individuals.[2,11]

Conventional resting-state functional connectivity analysis addresses the static nature of the coactivation of multiple brain areas. Here, it is presumed that the nature of interactions is stable over time, ie, during a recording session. In contrast, several approaches such as dynamic functional connectivity[13] and stochastic dynamic causal modeling,[14] address temporal dynamics of brain network interactions and the variation of interactions over time. These approaches provide further information complementary to conventional functional connectivity analysis. Using dynamic functional connectivity analysis, previous studies identified altered neural dynamics in CHR.[15,16] Energy landscape analysis is a data-driven method derived from statistical physics using the pairwise maximum entropy model (MEM) to estimate large-scale brain network dynamics such as frequency and duration and/or shift between different brain states.[17] In short, a brain state tends to go downhill being attracted by local minimum attractors (basins), whereas other times it goes uphill due to random fluctuations (paths and trajectories), and often shifts to another basin, forming an energy landscape.[18] The local minimum attractors (basins) could represent common mental states, and the temporal changes in whole-brain neural activity patterns (paths and trajectories) could be related to mental flexibility, together forming the mental set. Besides details of modeling approaches, the advantage of the energy landscape method over conventional dynamic functional connectivity analysis is the time resolution of dynamics. The conventional dynamic functional connectivity analysis requires substantial time points to calculate connectivity, and the long time window (often exceeding 20 s) works as a temporal smoothing to estimate the dynamics of brain network interactions.[13] In contrast, energy landscape analysis is capable to assign the state of brain dynamics for each individual time point, allowing it to address more precise dynamics of brain network interactions.[19] In addition, capturing higher time resolution of brain dynamics allows to assess metastable states in brain network interactions.[20] The optimal brain network dynamics traveling the energy landscape is important for healthy brain functioning, and is altered in psychiatric diseases, particularly in psychosis.[21] Thus, energy landscape analysis has the potential to determine relatively stable and dominant patterns of neural activity as local minima, as well as the dynamics of transition between the local minima in high-dimensional data without an a priori hypothesis.[19] Importantly, the energy landscape analysis method has recently been adopted to evaluate brain dynamics in clinical populations such as autism spectrum disorders[22], major depression,[23] epilepsy,[24] Alzheimer's disease,[25] or chronic schizophrenia.[21]

Neurocognitive deficits are regarded as a core component of psychosis,[26] and neurocognitive impairments often develop during the prodromal period and early after a first diagnosis of psychosis,[27–29] finally leading to a stable pattern of pronounced deficit in patients with chronic schizophrenia. Thus, with regard to neurocognitive functioning, the years prior to the onset of psychosis are critical. First-episode psychosis and CHR patients have impairments in various cognitive domains, including executive functioning, working memory, processing speed, verbal learning and memory, and premorbid intelligence quotient (IQ).[30] Amongst cognitive domains, verbal memory, and processing speed show the most significant deficits in CHR patients, and are associated with altered fronto-temporal functional and structural connectivity.[29–35] Based on our own previous work and the work of others, processing speed appears to have a key role in mediating other cognitive functions, being highly predictive for psychosis conversion.[29,31,35]

Therefore, we investigated resting-state brain network dynamics in adolescents and young adults with CHR and healthy controls (HC) using energy landscape analysis. We expected that RSN that are involved in aberrant salience and positive psychotic symptoms (eg, limbic and salience networks) would show increased likelihood (eg, increased duration/frequency and higher transition into states) of simultaneous activity, whereas RSN involved in optimal neurocognitive processing (eg, FPN, DAN)

would be deactivated/show lower likelihood of occurrence in psychosis/CHR patients compared to controls. Consecutively, we hypothesized that these brain states would show associations with positive symptoms (eg, hallucinations, delusions), processing speed and delayed recall of a verbal memory task.

Methods

Study Participants

Patients Fifty CHR (26 females, mean age 18.5 years) seeking help for mental problems at the Bern Early Recognition and Intervention Centre for Mental Crisis (FETZ Bern; www.upd.ch/fetz; for further details see[36]) between January 2019 and June 2021 were included in the study (table 1). All participants, and in the case of minors, their legal guardians with the child's assent, gave written informed consent for their coded clinical data to be used in scientific analyses and publications (Cantonal Ethics Committee Bern ID 2018-00951). The FETZ Bern is the only early detection and intervention center for psychosis in the Canton of Bern (1.035 mil population), Switzerland, screening approximately 80 patients per year (ages 8–40 years) according to European Psychiatric Association (EPA) guidelines.[3,4] The FETZ Bern targets persons with putative psychotic symptoms or CHR symptoms between 8 and 40 years of age. Exclusion criteria for a CHR state are (1) past clinical diagnosis of any psychotic disorder according to DSM and ICD, (2) diagnosis of delirium, dementia, amnestic or other neurological disorders, and (3) general medical conditions affecting the central nervous system. Subjects of the CHR group fulfilled at least one of the EPA criteria. Present DSM-IV non-substance-related axis-I disorders, including affective, anxiety, eating, somatoform, obsessive–compulsive, posttraumatic stress disorder, and substance use disorders were assessed using the Mini-International Neuropsychiatric Interviews (MINI/MINI-Kid[37,38]). At the time of first analysis of the data, the FETZ Bern recruitment of CHR patients was still ongoing.

Healthy Controls Thirty-three healthy participants (17 females, mean age 20.0) were included in the study (table 1). They were recruited via advertisements, and did not show any CHR criterion nor psychosis nor any other mental disorder according to ICD-10/DSM-IV. HC underwent the same psychopathological assessments as described for CHR patients.

Psychopathological and Neurocognitive Assessments

CHR Assessments CHR symptoms and criteria according to the EPA[3(p)] were employed as semi-structured clinical interviews. Two major sets of CHR criteria were used for the assessment of this state: (1) ultra-high risk (UHR) criteria, ie, attenuated (APS) or brief intermittent psychotic symptoms (BIPS) and genetic risk and functional decline (GRFD); and (2) basic symptom (BS) criteria, ie, cognitive disturbances (COGDIS) and cognitive-perceptive basic symptoms (COPER).[2,3] The two symptomatic UHR criteria APS and BIPS include positive symptoms of psychosis where some insight into their abnormal nature is still present.[39] BSs are subtle, subjectively experienced subclinical disturbances mainly in perception and cognition where insight is also present, which can usually be assessed from age 8 onwards.[40] UHR criteria[41] were evaluated with the Structured Interview for Psychosis-Risk Syndromes [SIPS][42] and the early version

Table 1. Demographic Data

	CHR	HC	*t*-value/Chi-squared	*P*-value
Number	50	33		
Age, years	18.5 (3.8)	20.0 (5.1)	−1.41	.161
Sex m/f	24/26	16/17	0.000	1
Highest ISCED (1/2/3/n.a)	1/36/10/3	6/12/14/1	14.35	.002
Medication y/n; CPx	8/42; 17.4 (56.0)	—		
SOFAS score	58.0 (12.3)	87.9 (4.1)	−13.25	<.001
SIPS P1	3.5 (1.2)	1.0 (0.4)	11.39	<.001
SIPS P2	2.4 (1.5)	0.1 (0.3)	8.37	<.001
SIPS P3	0.7 (1.1)	0.1 (0.2)	3.53	<.001
SIPS P4	3.4 (1.3)	0.2 (0.7)	12.80	<.001
SIPS P5	0.8 (1.0)	0.2 (0.6)	2.89	.004
SIPS pos total	10.8 (3.7)	1.6 (1.4)	13.50	<.001
VLMT del. rec.	48.4 (31.7)	60.2 (27.5)	−1.71	.092
DST	72.0 (18.9)	85.0 (19.5)	−3.16	.002

Note: CHR, clinical high risk; HC, healthy controls, age in years, sex m, male; f, female; ISCED, international standard classification of education, levels 1/2/3/not applicable. Antipsychotic medication: number yes/no; CPx, chlorpromazine equivalents (mean ± sd); SOFAS, social and occupational functioning; SIPS, structured interview for psychosis-risk syndromes, positive symptoms scores (P1–P5); VLMT, verbal learning and memory test, percentiles; del. rec., delayed recall (after 20 min); DST, digit symbol substitution test, number correct.

of the Comprehensive Assessment of At-Risk Mental States [CAARMS].[43] The SIPS/CAARMS assesses the presence of APS, BIPS, and GRFD.

Basic symptom criteria[44] including COPER and COGDIS were assessed using the Schizophrenia Proneness Instruments (SPI-A/SPI-CY).[45,46] The basic symptoms are self-experienced subclinical disturbances in thought, speech and perception, that are barely perceived by others. The basic symptom criteria are 14 such disturbances that can be allocated to COGDIS and/or COPER. Additionally, the Mini-International Neuropsychiatric Interview (MINI) for adults[37] and its version for children[38] were used to assess DSM-IV diagnoses. All interviewers underwent intensive training for 3 months prior to diagnosing patients according to the respective criteria and continuing supervision of ratings during the diagnostic process from co-author CM.

Neuropsychological Assessment The neurocognitive battery in the FETZ Bern examines neurocognitive domains which have previously been found to be impaired in CHR and psychotic patients.[36,47] For the present study, age-adjusted norms for the following assessments were used.

To assess verbal memory, the German version of the Verbal Learning and Memory Test (VLMT)[48] was used. The VLMT is a brief, easily administered, pencil-and-paper measure evaluating immediate memory span, learning capacity, susceptibility to interference, and recognition memory. It consists of 15 nouns (List A) that are read aloud for five consecutive trials (Trial 1: immediate memory span), and each trial is followed by a free-recall test. On completion of Trial 5 (Trials 1–5: learning capacity), an interference list of 15 words (List B) is presented, followed by a free-recall test of that list. Immediately after this, delayed recall of the first list is tested (Trial 6) without further presentation of the words. After a 20-min delay period, the participant was again required to recall words from List A (Trial 7). After this, a matrix array was tested, in which the individual must identify List A words from a list of 50 words (recognition memory) containing all items from List A and B and 20 words phonemically or semantically similar to those in List A and B. Correct answers are used as outcome variables (max. 15 in the Trials 1, 6, 7, List B, and recognition memory and max. 75 sum of Trials 1–5 [learning capacity]). For the present study, we focused on delayed recall (eg, in accordance with[33,49]).

Processing speed was measured using the Digit Symbol Substitution Test (DST),[50] a subtest of the WISC-IV[51] and WAIS-III.[52] The DST is a paper-pencil test in which subjects match symbols to numbers according to a key from 1 to 9. The task is to draw the symbols in boxes under numbers as fast and as accurately as possible. The number of correct symbols after 120 s is counted. The maximum number of correct symbols can be 119 for children and 133 for adults.

MRI Acquisition and Preprocessing

All MRI data was acquired by a 3T Siemens Prisma scanner (Siemens, Germany) with a customized 32-channel head coil. We acquired the whole-brain T1-weighted image by magnetization-prepared 2 rapid acquisition with gradient echo (MP2RAGE) sequence with following parameters: Echo time = 2.98 ms; repetition time = 5000 ms; Inversion time 1/2 = 700/2500 ms; flip angle 1/2 = 4/5°; number of slices = 176; field of view = 256 × 256 mm; slice thickness = 1mm; voxels size = 1 mm isotropic voxel.

Resting-state fMRI was acquired with T2*-weighted 2D multi-band echo planar imaging (EPI) with the following parameters: Echo time = 37 ms; repetition time = 1300 ms; flip angle = 52°; number of slices = 60; slice thickness = 2.2 mm; gap between slices = 0 mm; field of view = 230 × 230 mm; voxel size = 2.2 × 2.2 × 2.2 mm; multi-band acceleration factor = 4. We acquired 300 volumes for each subject. First five volumes are automatically discarded to achieve equilibrium of magnetization. While measuring resting-state fMRI, participants were instructed to open eyes and to "think about whatever comes to mind." To reduce the risk of falling asleep during resting-state fMRI measurement, we performed a resting-state fMRI scan at the beginning of the entire measurement (approx. 50 min).

We used SPM12 (Wellcome Department of Cognitive Neurology, https://www.fil.ion.ucl.ac.uk/spm/) and CAT12 toolbox (http://www.neuro.uni-jena.de/cat/)) for preprocessing of MRI data. Using CAT12 toolbox, we first segmented a T1 image into grey matter (GM), white matter (WM), and cerebrospinal fluid (CSF) images in the native space as well as obtained parameters to normalize the native T1 image to the standard brain of the Montreal Neurological Institute (MNI) space. Then, EPI images are realigned to the first image to correct for head movements in the scanner, and then applied slice timing correction. The corrected EPI images were coregistered to anatomical T1 image in the native space and normalized into the MNI space using parameters obtained from the T1 image processing. We applied spatial smoothing to the normalized images (2 mm isotropic voxel) with a Gaussian kernel of full-width half-maximum at 6 mm. We also normalized the segmented GM image to individually specify voxels in the GM for extraction of blood oxygen level-dependent (BOLD) time series. Further, we also normalized the segmented CSF and WM images to extract the non-neural signals of CSF and WM regions.

fMRI Signal Extraction from Brain Networks

We extracted the time series of BOLD from 400 regions of interest (ROIs) defined in Schaefer2018_Parcellations and classified them into seven functionally independent networks[53] (figure 1A), VIN, SMN, DAN, SAN, SAN, FPN, and DMN (figure 1B). The BOLD time course of

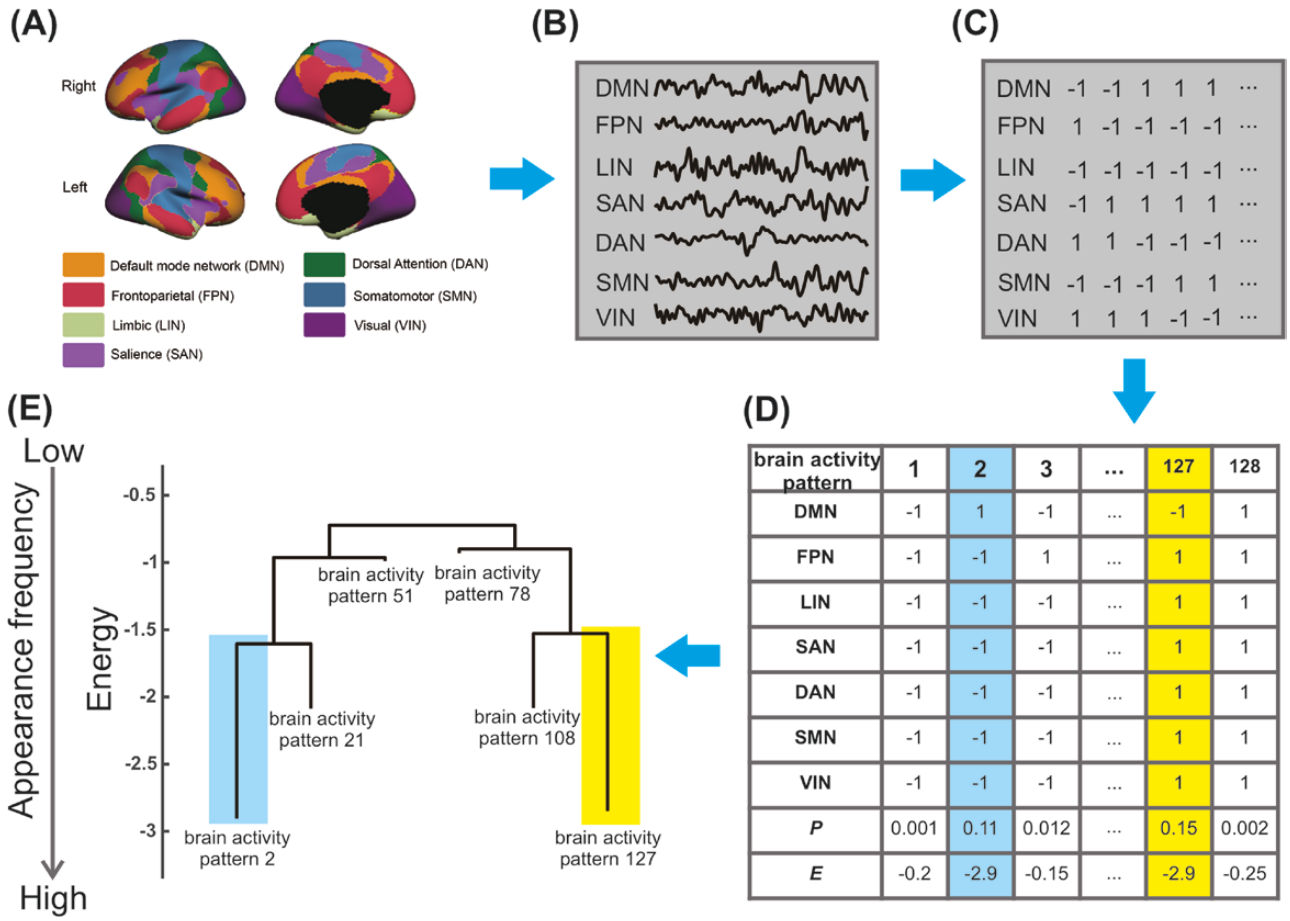

Fig. 1. Procedures of energy landscape analysis. (A) Region of interests (ROIs) from Schafer atlas[54], (B) BOLD signals of seven functionally different brain networks were extracted, and (C) they were binarized by the mean of each time series. (D) The distribution of the frequency of activity patterns is fitted by a pairwise MEM model, and (E) the energy landscape is constructed from the MEM model.

each network is calculated by averaging BOLD signal time courses in the 400 ROIs corresponding to each network. To remove non-neural signal sources from the BOLD time course of the seven networks, we used linear regression with nine regression parameters, including six motion parameters, average signals over the CSF, WM, and whole-brain. To create subject-specific CSF and WM masks, the subject-specific normalized CSF and WM images were thresholded at 0.95 (95% of the posterior probability of CSF or WM, respectively). Then, the subject-specific whole-brain mask was created by adding the subject-specific CSF, WM, and GM images and thresholding at 0.95. Finally, we performed band-pass temporal filtering (0.01–0.1 Hz). Although scrubbing EPI volumes to remove those with excessive head movement (censoring based on frame-wise displacement) is recognized as beneficial for correlation measures in functional connectivity analysis, the impact of head movement has yet to be investigated in energy landscape analysis. Furthermore, we implemented global signal regression to minimize the influence of head movement. Therefore, we did not employ scrubbing in our current analysis.

Pairwise MEM Fitting

We fitted the pairwise MEM to the preprocessed fMRI data according to previous studies[17,19,22,55] by using the Energy Landscape Analysis Toolkit (https://sites.google.com/site/ezakitakahiro/software).[19] For each network BOLD time course of each participant, we binarized the BOLD time course thresholded at its average value. Here, we regarded the BOLD activity larger/smaller than the time-averaged threshold as active/inactive (+1/0) (figure 1C). We then concatenated those binarized BOLD signals from all participants in the same group for each network activity. In this method, the activity pattern at time t in each network i is specified by a N-dimensional binary vector $V^t = \left[\sigma_1^t, \sigma_2^t, \ldots, \sigma_i^t, \ldots, \sigma_N^t\right]^T$ where σ_i^t is the binarized activity (either active [+1] or inactive [0]) and N (= 7) is the number of the networks. Note that the number of possible activity patterns is 2^N and that the kth brain activity pattern is described by V_k (k = 1, 2, . . . , 2^N). In the MEM, the frequency of the brain activity pattern V_k obeys the Boltzmann distribution[56] (figure 1D), $P(V_k) = e^{-E(V_k)} / \sum_{l=1}^{2^N} e^{-E(V_l)}$, where $E(V_k)$

represents the energy for activity pattern V_k defined by $E(V_k) = -\sum_{i=1}^{N} h_i\sigma_i - (1/2)\sum_{i=1}^{N}\sum_{j=1}^{N} J_{ij}\sigma_i\sigma_j$.

Here, we calculated h_i and J_{ij} by maximum likelihood estimation to adjust the model-based activation of network i, $\langle\sigma_i\rangle_{\text{model}}$ and the model-based pairwise interaction between networks i and j, $\langle\sigma_i\sigma_j\rangle_{\text{model}}$ toward the empirical activation of network i and j, $\langle\sigma_i\sigma_j\rangle$, respectively. Here, $\langle\sigma_i\rangle_{\text{model}} = \sum_{i=1}^{N}\sigma_i(V_l)P(V_l)$ and $\langle\sigma_i\sigma_j\rangle_{\text{model}} = \sum_{l=1}^{2^N}\sigma_i(V_l)\sigma_j(V_l)P(V_l)$. Note that this energy value does not mean any biological energy. It is rather a statistical index, which indicates the occurrence probability of each brain activity pattern. That is, activity patterns with lower energy values tend to occur more frequently.

After fitting the data to the pairwise MEM model, we calculated two metrics to evaluate goodness of fit. First, we calculated the accuracy measure in the same manner as the previous studies.[19,22,55]

$$r_D = (D_1 - D_2)/D_1$$

where D_1 and D_2 represent the Kullback–Leibler divergence between the MEM and data in the first-order model (the MEM is restricted to have no interaction term, ie, $J_{ij} = 0$ for all i and j) and in the second-order model (the MEM considering interaction term) respectively. We obtained $r_D = 1$ when the pairwise MEM perfectly reproduces the empirical distribution of activity patterns while $r_D = 0$ when the pairwise interaction does not contribute to improving the fitting. Second, we calculated Pearson's correlation coefficient between empirical appearance probability and model appearance probability $P(V_k)$ to evaluate the similarity of occurrence between the empirical data and fitted model.

Energy Landscape Analysis

We calculated the energy landscape (disconnectivity graph) as performed in previous studies[19,22,55] (figure 1E). The energy landscape is defined as a graph of brain activity patterns V_k with the corresponding energy $E(V_k)$ fitted in the pairwise MEM. Brain activity patterns are regarded as neighbors if they differ in only one active/inactive brain region. Then local minimums were identified as those activity patterns whose energy values were smaller than all of their neighboring patterns. Thus, local minimum patterns are more likely to appear than all their neighboring patterns. We exhaustively searched for local energy minima, then we summarized all brain activity patterns into local minimum basins, a family of brain activity patterns constituted by patterns neighboring to a local minimum pattern, in a data-driven manner. These basins were computed as follows: First, we select one network activity pattern, and evaluate if there is any neighboring pattern with a smaller energy value. If there is no neighboring pattern with a smaller energy value, we define the pattern as a local minimum pattern; otherwise, we search for a neighboring pattern with smaller energy. We iterate the search process until it reaches a local minimum pattern. We then assign the initial state to the basin of the local minimum. We iterated the procedure for all patterns in the pairwise MEM. In this way, we assigned all 2^N patterns to a single local minimum basin. For each branch of the dysconnectivity graph, we further categorized local minimum basins with higher occurrence into a major state (state 1 and state 2) and local minimum basin with lower occurrence into minor states (state 3 and 4) to perform direct comparisons between HC and CHR (figure 2).

Calculation of Representative Feature Metrics of the Energy Landscape Analysis

In the current study, we focused on the following three metrics that characterize the brain dynamics from the energy landscape analysis: Mean duration, occurrence, and transition frequency. The first parameter is the mean duration of each state, representing how long each state continues. For each state, we averaged the duration of all appearances. The second parameter is the occurrence of the brain state, representing how often each brain state happens per second. The number of occurrences is divided by the entire length of the resting-state fMRI session (390 s). The third parameter is the transition frequency, which shows how many times a brain state transits from one brain state to another brain state per one time step. The number of each transition type is divided by the entire time points of the resting-state fMRI session (300). These three metrics are calculated for each participant based on the group-level energy landscape. Then, we compared these parameters between the groups.

Associations Between Brain Dynamics and Symptoms and Cognition

To investigate how brain dynamics were associated with psychopathological and neuropsychological measures, we calculated Spearman's rank correlation coefficients between three brain dynamics parameters and SIPS total scores in the CHR group, exclusively. Further, we calculated Spearman correlations with the VLMT delayed recall and the DST. Here, results are reported uncorrected and false discovery (FDR) corrected for multiple comparisons.

Random-Walk Simulation of Brain Dynamics

To validate the characteristics of the brain dynamics acquired from the empirical data, we performed a random-walk simulation in the energy landscape as performed in previous studies.[19,22,55] We numerically simulated the

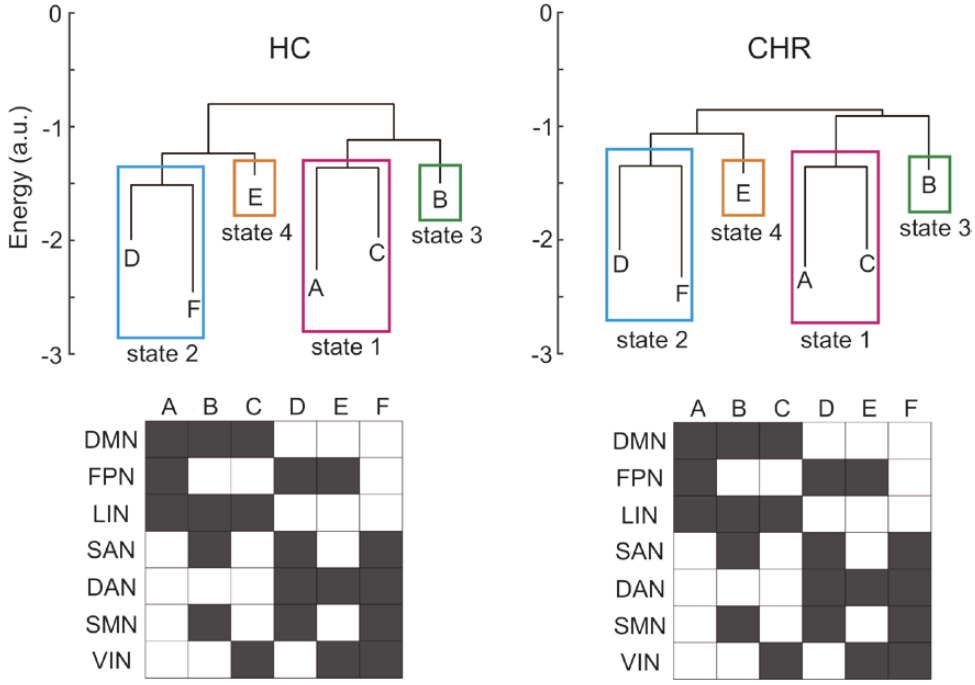

Fig. 2. Identifications of the local minimum and the comparison of the energy-landscape structures. (Upper) Disconnectivity graphs of energy-landscape structure. Lower energy reflects more stable and more frequent occurrence of a local minimum pattern, while higher energy reflects less stable and less frequent occurrence. (Bottom) The activity patterns corresponding to local minimum described in the disconnectivity graphs. Both disconnectivity graphs and brain activity patterns of local minimum are identical between HC and CHR (bottom). Based on the similar hierarchal structures of the energy landscapes across the groups, we summarized the local minima A and C to the major state 1 (magenta) and the local minima D and F to the major state 2 (cyan). Furthermore, we summarized the local minimum B to the minor state 3 (green), and the local minimum E to the minor state 4 (orange).

movement of the brain activity patterns using a Markov chain Monte Carlo method with the Metropolis–Hastings algorithm.[57,58] In this method, any brain activity pattern V_i could move only to a neighboring pattern V_j with probability $P_{ij} = \min\left[1, e^{E(V_i)-E(V_j)}\right]$ derived from the pairwise MEM model. For each group, we performed a single session of the random-walk simulation with 10^8steps. An initial pattern was randomly chosen, and the time trajectory of activity patterns was obtained. Then, the activity patterns were assigned to the brain states constituted by local minimum basins. For each group, we calculated the three classes of parameters (mean duration, occurrence, and direct transition frequencies), as described in "Calculation of representative feature metrics of the energy landscape analysis". Finally, we compared these model-based parameters with those from the empirical data.

Statistical Analysis

To compare beha Patients and HC vioral, demographic, and neuroimaging data between the HC and CHR groups, we performed a two-sample *t*-test and Chi-square test. For the association between neuroimaging and clinical data in CHR, Pearson's correlation efficient was calculated. We corrected for multiple testing's with false discovery rate correction.

Results

Sample Demographics

Patients and HC did not differ in sex or age (table 1). Eight CHR patients (16%) were on antipsychotic medication. Psychosocial functioning was significantly lower in CHR than in HC ($P < .001$). Significant differences were detected in SIPS scores and cognitive performance (overall univariate models, see table 1). SIPS positive total scores were significantly higher in CHR than in HC ($P < .001$). Similarly, DST performance was significantly lower in CHR than in HC ($P = .002$). Finally, delayed recall in VLMT was not significantly different between CHR and HC, but close to significant ($P = .09$).

Accuracy of Fitting of a Pairwise MEM to fMRI Data

We first evaluated the validity of the pairwise MEM model fitting for each group. We found a high accuracy of models fitted to the empirical fMRI data for HC and CHR (HC: 97.1%, CHR: 98.0%). This high accuracy of model fitting was also confirmed by correlations between the probability of each brain activity pattern acquired from the empirical data and that numerically derived from the pairwise MEM model for HC and CHR groups (Supplementary figure S1). As shown in Supplementary figure S1, empirical and model-derived

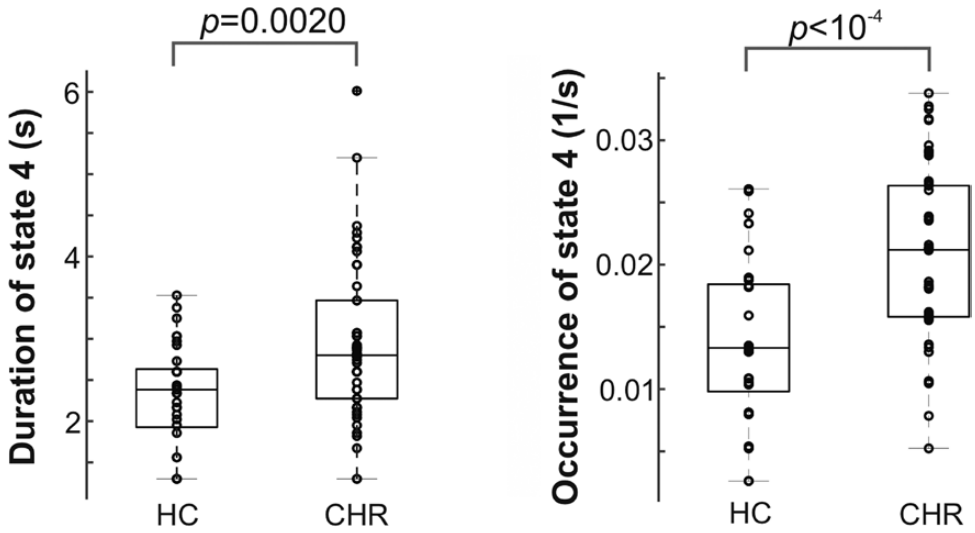

Fig. 3. Group comparison of the duration and occurrence of the brain states The duration (left) and occurrence (right) of state 4 were significantly longer and more frequent in CHR than in HC respectively (duration: $t(81) = -3.20$, $P = .0020$; occurrence: $t(81) = -4.20$, $P < .0001$).

occurrence probabilities of brain activity patterns are highly correlated ($r > .99$), indicating that the pairwise MEM was well fitted to the empirical fMRI data with high accuracy for HC and CHR groups.

Identification of Local Minimum Basins and the Comparison of the Energy Landscape Structures

Next, we identified local minimum brain activity patterns that constitute local minimum basins and their energy landscape (disconnectivity graph) for HC and CHR (figure 2). The local minimum brain activity patterns were identical between HC and CHR. Six local minimum basins (basin A–F) were identified in HC and CHR.

The disconnectivity graphs for the HC and CHR groups were also identical between HC and CHR. As shown in figure 2, each energy landscape had two main branches. One main branch of the disconnectivity graphs consisted of basin A, B, and C, while the other branch consisted of basin D, E, and F.

Each main branch also had two sub-branches. One sub-branch included two local minimums with lower energy (higher occurrence), while the other sub-branch included one local minimum with higher energy (lower occurrence). Based on such hierarchal characteristics and the similarity of the energy landscape structures across the two groups, we could consider the two pairs of the basins (higher occurrence) to be two main states, classifying basin A and C to main state 1, and basin D and F to main state 2. We also classified remaining local minimums with higher energy (lower occurrence) to minor states: basin B to state 3, and basin E to state 4 (figure 2). This simplification of the structures of energy landscapes allowed us to directly compare the characteristics of the brain dynamics across the groups.

Table 2. Association Between Energy Landscape Parameters and Clinical Scales

	Occurrence state 4	Duration state 4	Transition 2–4	Transition 4–1
SIPS pos. tot.	0.041	0.122	0.190	−0.033
VLMT del. rec.	−0.121	0.234	−0.328#	0.265
DST	−0.314#	0.048	−0.300#	−0.412*

Note: SIPS, standard interview for psychosis-risk syndromes, positive symptoms scores (p1–p5); VLMT, verbal learning and memory test, percentiles; del. rec., delayed recall (after 20 min); DST, digit symbol test.
*Survived FDR correction for multiple testing (P (FDR < .05)).
#$P < .05$ uncorrected for multiple comparison.

Characterization of the Brain Dynamics

We compared the mean duration and occurrence of each brain state in HC and CHR. As was shown in figure 3, the duration and occurrence of state 4 were significantly longer and higher in CHR than those in HC (two-sample t-test: $t(81) = 3.276$, $P = .0016$ and $t(81) = 4.247$, $P < .0001$, respectively). The random-walk simulation confirmed that the duration and occurrence of state 4 were longer in CHR than in HC (Supplementary figure S2).

We also compared the direct transition frequency among the brain states across the three groups (figure 4). We found that the direct transition frequencies from state 2 to state 4 and from state 4 to state 1 were significantly higher in CHR than in HC (two-sample t-test: $t(81) = 3.276$, $P = .0016$ and $t(81) = 3.867$, $P = 0.0002$, respectively). Furthermore, the random-walk simulation revealed that both of the direct transition frequencies

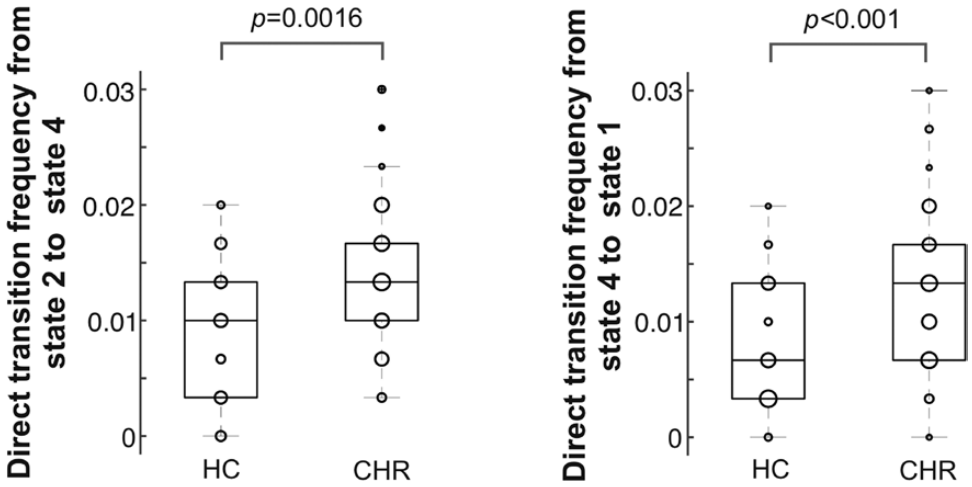

Fig. 4. Group comparison of the direct transition frequency across the brain states The direct transition frequency from state 2 to state 4 (left), and that from state 4 to state 1 (right) were significantly more frequent in CHR than in HC (the direct transition frequency from state 2 to state 4: $t(81) = -3.27$, $P = .0020$; the direct transition frequency from state 4 to state 1: $t(81) = -3.72$, $P \leq .001$ respectively).

(from state 2 to state 4, and from state 4 to state 1) were higher in CHR than in HC (Supplementary figure S3), validating the results of our empirical data.

Associations Between Brain Dynamics and Symptoms

Finally, we examined the association between brain dynamics and behavioral measures including psychopathological and neuropsychological assessments. We looked at the correlation of behavioral assessment with measures related to state 4 (occurrence, duration, and transition) in CHR. We found no significant correlations with total positive SIPS score ($P > .05$, table 2). In neuropsychological measures, significant correlations were detected between delayed recall of the VLMT and direct transition from state 2 to state 4 (P(uncorrected) = .023) (table 2). Further, significant correlations were detected with performance in the DST and transitions from state 2 to state 4 (P(uncorrected) = .036) and significant correlations between occurrence of state 4 (P(uncorrected) = .027), transition from state 2 to state 4 and transition from state 4 to state 1 (P(uncorrected) = .003) (table 2). However, only the correlation between transition of 4 to 1 and DST survived correction for multiple testing (P(FDR) = .039, figure 5, table 2). These results suggest that stronger attraction to state 4 is associated with more severe impairment in processing speed.

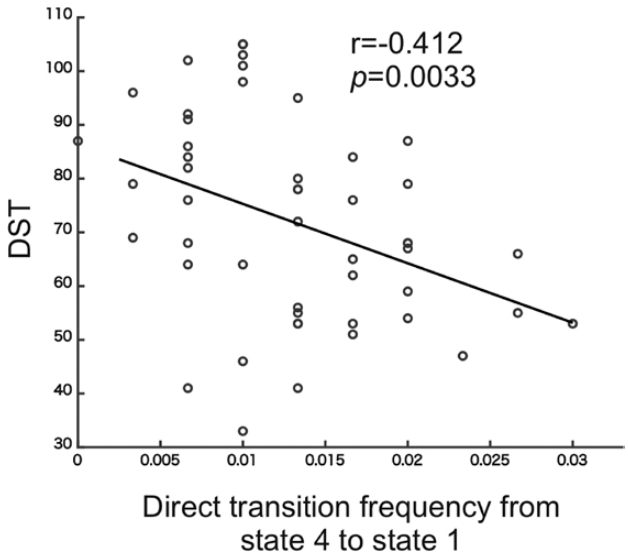

Fig. 5. Association between processing speed and energy landscape dynamics Scatter plot depicts the relationship between direct transition frequency from state 4 to 1 (X-axis) and processing speed measured by digit symbol test (DST) (Y-axis), showing significant negative correlation (P(FDR) = .039).

Discussion

This study addressed the temporal dynamics of brain networks by applying energy landscape analysis to resting-state fMRI data. A significantly longer duration and higher occurrence of state 4 in CHR as compared to HC was found. Further, transition from state 2 to state 4, as well as transition from state 4 to state 1 was significantly more frequent in CHR compared to HC.

The results suggest that brain dynamics in CHR tend to be attracted to state 4. Once the brain dynamics fall into state 4, they remain for a longer time in state 4. Importantly, state 4 is characterized by the deactivation of FPN, DAN, and VIN, and the activation of DMN, LIN, SAN, and SMN networks.

The significance of investigating brain network dynamics is uncovering the metastability of brain networks.[20] The dynamics of brain networks are fundamentally shaped by the structural connections of neural networks and the patterns of neuronal activity. In psychiatric illnesses, dysfunctional synaptic connections

may skew neural transmission within these networks. Consequently, such dysfunctional connections could lead to altered brain dynamics in psychiatric disorders. This alteration may manifest as either an extended or abbreviated duration of specific brain states or as changes in the propensity or frequency of transitions between brain states.

In addressing the dynamics of brain network interactions, dynamic functional connectivity analysis has been extensively utilized. A major limitation of conventional dynamic functional connectivity analysis is the necessity for a prolonged time window to compute the connectivity matrix, which results in a loss of the temporal resolution of the dynamics.[13] However, a recent advancement, known as leading eigenvector dynamics analysis (LEiDA), has overcome this limitation.[59] It extracts phase information from neural time series—particularly fMRI BOLD time series—and assigns phase lags between brain regions to determine dynamic functional connectivity. This method enables the estimation of dynamic functional connectivity at each time point, thereby providing a detailed temporal resolution of brain network dynamics, akin to energy landscape analysis. Despite these similarities, there is a significant distinction between the LEiDA approach and energy landscape analysis. LEiDA models the dynamics of whole-brain activity as an accumulation of bivariate interactions, whereas energy landscape analysis considers interactions among brain regions collectively to define the dynamics of whole-brain activity. Consequently, EL does not reduce whole-brain dynamics to a series of bivariate interactions but captures a more holistic and integral nature of whole-brain interactions within brain networks. However, EL is limited by the number of brain areas that can be included when estimating parameters for the pairwise MEM, whereas LEiDA offers scalability regarding the number of brain regions included.

Comparing the local minimum states of the energy landscape with correlations of the seven networks (Supplementary figure S4), strong positive and negative correlations ($|r| > .3$) were consistent with major states (states 1 and 2) of the energy landscape. In contrast, in state 4, the coactivation of DMN and SMN, coactivation of DMN and SAN, and the co-deactivation of FPN and VIN are inconsistent with correlations of resting-state networks, suggesting that these three interactions characterize minor states of network interactions, and prolonged state 4 reflects psychotic states including CHR.

Using a data-driven approach this finding strongly supports current hypotheses on the pathogenesis of psychosis.[8] Involvement of the salience,[60,61] limbic,[62] DMN,[10] or somatosensory networks[63] have separately been demonstrated in the pathophysiology of chronic schizophrenia. However, a coactivation of these RSNs has not been previously demonstrated, and never in CHR states. In CHR, we found brain dynamics are more frequently attracted to the minor state 4, and a more frequent transition from state 4 to state 1 was correlated with poorer performance of the DST. While these results might seem counterintuitive, it is important to note that brain states are transient and continuously fluctuate. Thus, an increased transition from state 4 to state 1 could be indicative of a more frequent occurrence of state 4. This observation suggests that not only the stability of brain states but also the dynamic transitions between them play a crucial role in understanding brain function and cognition. In particular, the minor states we observed by the energy landscape analysis were masked by the major states in conventional functional connectivity analysis. For instance, the DMN is typically anti-correlated with the SAN and SMN (Supplementary figure S4). However, coactivation of the DMN, SAN, and SMN is evident in state 4 (figure 2). This indicates that the brain's ability to switch between different states is potentially vital for cognitive functions, particularly processing speed, emphasizing the importance of neural flexibility, and adaptability. Among neurocognitive functions, processing speed shows the strongest impairments in people with psychosis, is a predictor of long-term psychosocial functionality, and has been associated with conversion to psychosis in CHR individuals.[29,64,65] More importantly, processing speed appears to be a superordinate factor controlling other cognitive domains and thus, may lie upstream of the generalized neurocognitive impairments seen in psychosis or CHR. Several authors have therefore suggested processing speed as a main target for cognitive treatment interventions.[65] Vice versa our data indicate that targeting brain dynamics may help to activate or modulate cognitive functions. In a therapeutic context, interventions targeting the modulation of specific brain states or their transitions could potentially be effective. However, our hypothesis of an association with positive symptoms was not confirmed in the present sample.

A meta-analysis of functional disconnection in schizophrenic patients revealed hyper-connectivity between the LIN and SAN networks.[66] While LIN and SAN might be involved in aberrant salience, the role of the DMN is less clear. DMN activity is deactivated during task performance, thus increased activation might contribute to cognitive impairments (eg, dream-like states).[10] The finding on the SMN is fitting to recent observations that motor symptoms are a reliable biomarker, can be detected early in psychosis development, and are independent of medication side effects, which is reflected in recent activities to include motor symptoms in the ICD-11 and the research domain criteria (RDoC) framework.[67–70]

An important note regarding methodological variations among previous studies in energy landscape analysis is the definition of brain networks. The current study and a study by Yamashita et al,[71] used the seven networks

of Schaefer's parcellation. In contrast, other studies used different parcellation, or focused on a particular brain structure such as subcortical structure, or DMN. In addition, the TR of the fMRI sequence also has a great impact on the time resolution of brain dynamics. While recent multi-band sequence measures less than a second TR, older data sets utilize TR longer than 2 s.[19]

Limitations of current study include the following: First, the cross-sectional analysis provided group differences, but the association between the onset of psychosis and the alteration related to state 4 is not established. Longitudinal data is required to address this question in future studies. In the CHR cohort, 16% of patients received antipsychotics, which could affect energy landscape metrics. Longitudinal follow-up is needed to how the current results could impact on long-term clinical outcomes, such as conversion. Moreover, with regard to symptomatic and cognitive measures, only DST but not VLMT survived correction for multiple testing, which dampens the generalizability/validity of these results.

The lack of a first-episode psychosis group is another limitation of our study. However, with regard to CHR status, the most recent meta-analysis indicated 35% of CHR individuals convert to full-blown psychosis within a 10-year period.[5] Thus, we predict that about 17 individuals in our CHR group would convert to full-blown psychosis in the long term. Importantly, from those CHR individuals who do not convert to psychosis, only a minority of 7%–25% will remit at follow-up. In contrast more than 75% will suffer from continuing attenuated psychotic symptoms, deterioration of pre-existing mental disorders with significant functional impairments, and/or newly emerging non-psychotic mental disorders such as bipolar disorder, substance use, or borderline disorder.[72] These observations have led to the recent adaptation of a broader clinical high at-risk mental state (CHARMS) model supporting the view that CHR is a pluripotent and heterotopic early marker for severe mental disorders.[73,74] This view is in line with transdiagnostic and/or dimensional approaches to psychiatry, such as the "Research Domain Criteria" (RDoC, NIMH)[75] and the Hierarchical Taxonomy of Psychopathology (HiTOP).[76] The finding of involvement of limbic and salience systems and of the DMN in a brain state more frequently observed in help-seeking CHR patients does well integrate with a transdiagnostic view as these resting-state networks seem to be involved in several mental disorders.[77–79] Thus, longitudinal studies of larger samples will have to clarify whether our findings are specific for psychosis or, rather, are a marker of general psychopathology indicative of various mental disorders.

Conclusions

In CHR, a brain state with coactivation of RSNs that are involved in aberrant salience and other positive symptoms may occur more frequently and remain for longer time periods. The same brain state is characterized by the deactivation of RSN involved in cognition, and was negatively associated with processing speed in CHR. The current study provides new perspectives on CHR that aberrant brain dynamics in CHR account for the impairment of core cognitive functions in CHR.

Supplementary Material

Supplementary data are available at *Schizophrenia Bulletin Open* online.

Acknowledgments

JK and YM are supported by Swiss National Foundation (192623). TY is supported by KAKENHI (JP18K15491). All authors declare no conflict of interest.

References

1. GBD 2019 Mental Disorders Collaborators, Global, regional, and national burden of 12 mental disorders in 204 countries and territories, 1990–2019: a systematic analysis for the Global Burden of Disease Study 2019. *Lancet Psychiatry.* 2022;9(2):137–150. doi:10.1016/S2215-0366(21)00395-3
2. Fusar-Poli P, Borgwardt S, Bechdolf A, *et al.* The psychosis high-risk state: a comprehensive state-of-the-art review. *JAMA Psychiatry.* 2013;70(1):107–120. doi:10.1001/jamapsychiatry.2013.269
3. Schultze-Lutter F, Michel C, Schmidt SJ, *et al.* EPA guidance on the early detection of clinical high risk states of psychoses. *Eur Psychiatry.* 2015;30(3):405–416. doi:10.1016/j.eurpsy.2015.01.010
4. Schmidt SJ, Schultze-Lutter F, Schimmelmann BG, *et al.* EPA guidance on the early intervention in clinical high risk states of psychoses. *Eur Psychiatry.* 2015;30(3):388–404. doi:10.1016/j.eurpsy.2015.01.013
5. Salazar de Pablo G, Radua J, Pereira J, *et al.* Probability of transition to psychosis in individuals at clinical high risk: an updated meta-analysis. *JAMA Psychiatry.* 2021;78(9):970–978. doi:10.1001/jamapsychiatry.2021.0830
6. Kindler J, Schultze-Lutter F, Hauf M, *et al.* increased striatal and reduced prefrontal cerebral blood flow in clinical high risk for psychosis. *Schizophr Bull.* 2018;44(1):182–192. doi:10.1093/schbul/sbx070
7. Jalbrzikowski M, Hayes RA, Wood SJ, *et al.* Thinner cortex is associated with psychosis onset in individuals at clinical high risk for developing psychosis: an ENIGMA Working Group Mega-Analysis. Psychiatry and Clinical Psychology; 2021. doi:10.1101/2021.01.05.20248768
8. Friston K, Brown HR, Siemerkus J, Stephan KE. The dysconnection hypothesis. *Schizophr Res.* 2016;176(2–3):83–94. doi:10.1016/j.schres.2016.07.014
9. van den Heuvel MP, Hulshoff Pol HE. Exploring the brain network: a review on resting-state fMRI functional connectivity. *Eur Neuropsychopharmacol.* 2010;20(8):519–534. doi:10.1016/j.euroneuro.2010.03.008
10. Kindler J, Jann K, Homan P, *et al.* Static and dynamic characteristics of cerebral blood flow during the resting state in schizophrenia. *Schizophr Bull.* 2015;41(1):163–170. doi:10.1093/schbul/sbt180

11. Del Fabro L, Schmidt A, Fortea L, *et al.* Functional brain network dysfunctions in subjects at high-risk for psychosis: a meta-analysis of resting-state functional connectivity. *Neurosci Biobehav Rev.* 2021;128:90–101. doi:10.1016/j.neubiorev.2021.06.020
12. Ripke S, Neale BM, Corvin A, *et al.* Biological insights from 108 schizophrenia-associated genetic loci. *Nature.* 2014;511(7510):421–42+. doi:10.1038/nature13595
13. Hutchison RM, Womelsdorf T, Allen EA, *et al.* Dynamic functional connectivity: promise, issues, and interpretations. *Neuroimage.* 2013;80:360–378. doi:10.1016/j.neuroimage.2013.05.079
14. Daunizeau J, Stephan KE, Friston KJ. Stochastic dynamic causal modelling of fMRI data: should we care about neural noise? *Neuroimage.* 2012;62(1):464–481. doi:10.1016/j.neuroimage.2012.04.061
15. Mennigen E, Fryer SL, Rashid B, *et al.* Transient patterns of functional dysconnectivity in clinical high risk and early illness schizophrenia individuals compared with healthy controls. *Brain Connect.* 2019;9(1):60–76. doi:10.1089/brain.2018.0579
16. Du Y, Fryer SL, Fu Z, *et al.* Dynamic functional connectivity impairments in early schizophrenia and clinical high-risk for psychosis. *Neuroimage.* 2018;180:632–645. doi:10.1016/j.neuroimage.2017.10.022
17. Watanabe T, Masuda N, Megumi F, Kanai R, Rees G. Energy landscape and dynamics of brain activity during human bistable perception. *Nat Commun.* 2014;5(1):4765. doi:10.1038/ncomms5765
18. Watanabe T, Hirose S, Wada H, *et al.* Energy landscapes of resting-state brain networks. *Front Neuroinform.* 2014;8:1. doi: 10.3389/fninf.2014.00012
19. Ezaki T, Watanabe T, Ohzeki M, Masuda N. Energy landscape analysis of neuroimaging data. *Philos Trans Ser A Math Phys Eng Sci.* 2017;375(2096):20160287. doi:10.1098/rsta.2016.0287
20. Heitmann S, Breakspear M. Putting the "dynamic" back into dynamic functional connectivity. *Network Neurosci.* 2018;2(2):150–174. doi:10.1162/netn_a_00041
21. Braun U, Harneit A, Pergola G, *et al.* Brain network dynamics during working memory are modulated by dopamine and diminished in schizophrenia. *Nat Commun.* 2021;12(1):3478. doi:10.1038/s41467-021-23694-9
22. Watanabe T, Rees G. Brain network dynamics in high-functioning individuals with autism. *Nat Commun.* 2017;8(1):16048. doi:10.1038/ncomms16048
23. Regonia PR, Takamura M, Nakano T, *et al.* Modeling heterogeneous brain dynamics of depression and melancholia using energy landscape analysis. *Front Psychiatry.* 2021;12:780997. doi:10.3389/fpsyt.2021.780997
24. Krzemiński D, Masuda N, Hamandi K, Singh KD, Routley B, Zhang J. Energy landscape of resting magnetoencephalography reveals fronto-parietal network impairments in epilepsy. *Netw Neurosci (Cambridge, Mass.).* 2020;4(2):374–396. doi:10.1162/netn_a_00125
25. Klepl D, He F, Wu M, Marco MD, Blackburn DJ, Sarrigiannis PG. Characterising Alzheimer's disease with EEG-based energy landscape analysis. *IEEE J Biomed Health Inform.* 2022;26(3):992–1000. doi:10.1109/JBHI.2021.3105397
26. Barch DM, Ceaser A. Cognition in schizophrenia: core psychological and neural mechanisms. *Trends Cogn Sci.* 2012;16(1):27–34. doi:10.1016/j.tics.2011.11.015
27. Seidman LJ, Shapiro DI, Stone WS, *et al.* Association of neurocognition with transition to psychosis: baseline functioning in the second phase of the North American Prodrome Longitudinal Study. *JAMA Psychiatry.* 2016;73(12):1239–1248. doi:10.1001/jamapsychiatry.2016.2479
28. de Paula AL, Hallak JE, Maia-de-Oliveira JP, Bressan RA, Machado-de-Sousa JP. Cognition in at-risk mental states for psychosis. *Neurosci Biobehav Rev.* 2015;57:199–208. doi:10.1016/j.neubiorev.2015.09.006
29. Michel C, Ruhrmann S, Schimmelmann BG, Klosterkotter J, Schultze-Lutter F. A stratified model for psychosis prediction in clinical practice. *Schizophr Bull.* 2014;40(6):1533–1542. doi:10.1093/schbul/sbu025
30. Catalan A, Salazar de Pablo G, Aymerich C, *et al.* Neurocognitive functioning in individuals at clinical high risk for psychosis: a systematic review and meta-analysis. *JAMA Psychiatry.* 2021;78:859–867. doi:10.1001/jamapsychiatry.2021.1290
31. Büetiger JR, Michel C, Kaess M, Kindler J. Childhood maltreatment and its association with cognitive ability in young people suspected to be at clinical high risk of psychosis. *Psychopathology.* 2022;56:17–28. doi:10.1159/000524947
32. Seabury RD, Cannon TD. Memory impairments and psychosis prediction: a scoping review and theoretical overview. *Neuropsychol Rev.* 2020;30(4):521–545. doi:10.1007/s11065-020-09464-2
33. Antoniades M, Schoeler T, Radua J, *et al.* Verbal learning and hippocampal dysfunction in schizophrenia: a meta-analysis. *Neurosci Biobehav Rev.* 2018;86:166–175. doi:10.1016/j.neubiorev.2017.12.001
34. Klauser P, Cropley VL, Baumann PS, *et al.* White matter alterations between brain network hubs underlie processing speed impairment in patients with schizophrenia. *Schizophr Bull Open.* 2021;2(1):sgab033. doi:10.1093/schizbullopen/sgab033
35. Kochunov P, Coyle TR, Rowland LM, *et al.* Association of white matter with core cognitive deficits in patients with schizophrenia. *JAMA Psychiatry.* 2017;74(9):958–966. doi:10.1001/jamapsychiatry.2017.2228
36. Michel C, Kaess M, Flückiger R, *et al.* The Bern Early Recognition and Intervention Centre for mental crisis (FETZ Bern)—an 8-year evaluation. *Early Interv Psychiatry.* 2021;16:289–301. doi:10.1111/eip.13160
37. Sheehan DV, Lecrubier Y, Sheehan KH, *et al.* The Mini-International Neuropsychiatric Interview (M.I.N.I.): the development and validation of a structured diagnostic psychiatric interview for DSM-IV and ICD-10. *J Clin Psychiatry.* 1998;59(Suppl 20):22–33; quiz 34. quiz3457.
38. Sheehan DV, Sheehan KH, Shytle RD, *et al.* Reliability and validity of the Mini International Neuropsychiatric Interview for Children and Adolescents (MINI-KID). *J Clin Psychiatry.* 2010;71(3):313–326. doi:10.4088/JCP.09m05305whi
39. Flückiger R, Michel C, Grant P, *et al.* The interrelationship between schizotypy, clinical high risk for psychosis and related symptoms: cognitive disturbances matter. *Schizophr Res.* 2019;210:188–196. doi:10.1016/j.schres.2018.12.039
40. Fux L, Walger P, Schimmelmann BG, Schultze-Lutter F. The Schizophrenia Proneness Instrument, Child and Youth version (SPI-CY): practicability and discriminative validity. *Schizophr Res.* 2013;146(1–3):69–78. doi:10.1016/j.schres.2013.02.014
41. Yung AR, Stanford C, Cosgrave E, *et al.* Testing the ultra high risk (prodromal) criteria for the prediction of psychosis in a clinical sample of young people. *Schizophr Res.* 2006;84(1):57–66. doi:10.1016/j.schres.2006.03.014

42. McGlashan T, Cannon TD, Walsh B, Woods S. *The Psychosis-Risk Syndrome: Handbook for Diagnosis and Follow-Up*. Oxford, New York: Oxford University Press; 2010.
43. Yung AR, Yuen HP, McGorry PD, *et al.* Mapping the onset of psychosis: the comprehensive assessment of at-risk mental states. *Aust N Z J Psychiatry.* 2005;39(11–12):964–971. doi:10.1080/j.1440-1614.2005.01714.x
44. Schultze-Lutter F, Debbané M, Theodoridou A, *et al.* Revisiting the basic symptom concept: toward translating risk symptoms for psychosis into neurobiological targets. *Front Psychiatry.* 2016;7:9. doi:10.3389/fpsyt.2016.00009
45. Schultze-Lutter F, Addington J, Ruhrmann S, Klosterkötter J. *Schizophrenia Proneness Instrument, Adult Version (SPI-A)*. Rome: Fioriti; 2007.
46. Schultze-Lutter F, Marshall M, Koch E. *Schizophrenia Proneness Instrument, Child and Youth (SPI-CY)—Extended English Translation (EET)*. Rome: Fioriti; 2012. https://www.fioritieditore.com/prodotto/schizophrenia-proneness-instrument-child-and-youth-spi-cy-extended-english-version-2/. Accessed April 4, 2019.
47. De Herdt A, Wampers M, Vancampfort D, *et al.* Neurocognition in clinical high risk young adults who did or did not convert to a first schizophrenic psychosis: a meta-analysis. *Schizophr Res.* 2013;149(1–3):48–55. doi:10.1016/j.schres.2013.06.017
48. Dunn LM, Dunn DM. *PPVT-4: Peabody Picture Vocabulary Test*. 4th ed. Minneapolis, MN: Pearson Assessments. 2007.
49. Thygesen JH, Presman A, Harju-Seppänen J, *et al.* Genetic copy number variants, cognition and psychosis: a meta-analysis and a family study. *Mol Psychiatry.* 2021;26:5307–5319. doi:10.1038/s41380-020-0820-7
50. Jaeger J. Digit symbol substitution test: the case for sensitivity over specificity in neuropsychological testing. *J Clin Psychopharmacol.* 2018;38(5):513–519. doi:10.1097/JCP.0000000000000941
51. Wechsler D. *Wechsler Intelligence Scale for Children*. 4th ed. Minneapolis, MN: Pearson Assessment. 2012. doi:10.1037/t15174-000
52. Wechsler D. *Wechsler Adult Intelligence Scale*. San Antonio, Texas: The Psychological Corporation; 1997.
53. Braun U, Schäfer A, Walter H, *et al.* Dynamic reconfiguration of frontal brain networks during executive cognition in humans. *Proc Natl Acad Sci USA.* 2015;112(37):11678–11683. doi:10.1073/pnas.1422487112
54. Schaefer A, Kong R, Gordon EM, *et al.* Local-Global parcellation of the human cerebral cortex from intrinsic functional connectivity MRI. *Cereb Cortex*. 2018;28(9):3095–3114. doi:10.1093/cercor/bhx179
55. Ezaki T, Sakaki M, Watanabe T, Masuda N. Age-related changes in the ease of dynamical transitions in human brain activity. *Hum Brain Mapp.* 2018;39(6):2673–2688. doi:10.1002/hbm.24033
56. Jaynes ET. Information theory and statistical mechanics. II. *Phys Rev.* 1957;108(2):171–190. doi:10.1103/PhysRev.108.171
57. Hastings WK. Monte Carlo sampling methods using Markov chains and their applications. *Biometrika.* 1970;57(1):97–109. doi:10.1093/biomet/57.1.97
58. Metropolis N, Rosenbluth AW, Rosenbluth MN, Teller AH, Teller E. Equation of state calculations by fast computing machines. *J Chem Phys.* 1953;21:1087. doi:10.2172/4390578
59. Deco G, Cruzat J, Cabral J, *et al.* Awakening: predicting external stimulation to force transitions between different brain states. *Proc Natl Acad Sci USA.* 2019;116(36):18088–18097. doi:10.1073/pnas.1905534116
60. Palaniyappan L, Simmonite M, White TP, Liddle EB, Liddle PF. Neural primacy of the salience processing system in schizophrenia. *Neuron.* 2013;79(4):814–828. doi:10.1016/j.neuron.2013.06.027
61. Mallikarjun PK, Lalousis PA, Dunne TF, *et al.* Aberrant salience network functional connectivity in auditory verbal hallucinations: a first episode psychosis sample. *Transl Psychiatry.* 2018;8(1):69. doi:10.1038/s41398-018-0118-6
62. Walther S, Lefebvre S, Conring F, *et al.* Limbic links to paranoia: increased resting-state functional connectivity between amygdala, hippocampus and orbitofrontal cortex in schizophrenia patients with paranoia. *Eur Arch Psychiatry Clin Neurosci.* 2022;272:1021–1032. doi:10.1007/s00406-021-01337-w
63. Walther S, Schappi L, Federspiel A, *et al.* Resting-state hyperperfusion of the supplementary motor area in Catatonia. *Schizophr Bull.* 2017;43(5):972–981. doi:10.1093/schbul/sbw140
64. Mathias SR, Knowles EEM, Barrett J, *et al.* The processing-speed impairment in psychosis is more than just accelerated aging. *Schizophr Bull.* 2017;43(4):814–823. doi:10.1093/schbul/sbw168
65. Randers L, Jepsen JRM, Fagerlund B, *et al.* Generalized neurocognitive impairment in individuals at ultra-high risk for psychosis: the possible key role of slowed processing speed. *Brain Behav.* 2021;11(3):e01962. doi:10.1002/brb3.1962
66. Dong D, Wang Y, Chang X, Luo C, Yao D. Dysfunction of large-scale brain networks in schizophrenia: a meta-analysis of resting-state functional connectivity. *Schizophr Bull.* 2018;44(1):168–181. doi:10.1093/schbul/sbx034
67. Hirjak D, Meyer-Lindenberg A, Kubera KM, Thomann PA, Wolf RC. Motor dysfunction as research domain in the period preceding manifest schizophrenia: a systematic review. *Neurosci Biobehav Rev.* 2018;87:87–105. doi:10.1016/j.neubiorev.2018.01.011
68. Walther S, van Harten PN, Waddington JL, *et al.* Movement disorder and sensorimotor abnormalities in schizophrenia and other psychoses—European consensus on assessment and perspectives. *Eur Neuropsychopharmacol.* 2020;38:25–39. doi:10.1016/j.euroneuro.2020.07.003
69. Kindler J, Schultze-Lutter F, Michel C, *et al.* Abnormal involuntary movements are linked to psychosis-risk in children and adolescents: results of a population-based study. *Schizophr Res.* 2016;174(1–3):58–64. doi:10.1016/j.schres.2016.04.032
70. Nadesalingam N, Lefebvre S, Alexaki D, *et al.* The behavioral mapping of psychomotor slowing in psychosis demonstrates heterogeneity among patients suggesting distinct pathobiology. *Schizophr Bull.* 2022;49:sbac170. doi:10.1093/schbul/sbac170
71. Yamashita A, Rothlein D, Kucyi A, Valera EM, Esterman M. Brain state-based detection of attentional fluctuations and their modulation. *Neuroimage.* 2021;236:118072. doi:10.1016/j.neuroimage.2021.118072
72. Lin A, Wood SJ, Nelson B, Beavan A, McGorry P, Yung AR. Outcomes of nontransitioned cases in a sample at ultra-high risk for psychosis. *AJP.* 2015;172(3):249–258. doi:10.1176/appi.ajp.2014.13030418
73. Hartmann JA, McGorry PD, Destree L, *et al.* Pluripotential risk and clinical staging: theoretical considerations and preliminary data from a transdiagnostic risk identification approach. *Front Psychiatry.* 2021;11:553578. doi:10.3389/fpsyt.2020.553578
74. McGorry PD, Hartmann JA, Spooner R, Nelson B. Beyond the "at risk mental state" concept: transitioning to

transdiagnostic psychiatry. *World Psychiatry.* 2018;17(2):133–142. doi:10.1002/wps.20514

75. Insel T, Cuthbert B, Garvey M, *et al.* Research Domain Criteria (RDoC): toward a new classification framework for research on mental disorders. *Am J Psychiatry.* 2010;167(7):748–751. doi:10.1176/appi.ajp.2010.09091379
76. Kotov R, Krueger R, Watson D, *et al.* The Hierarchical Taxonomy of Psychopathology (HiTOP): a dimensional alternative to traditional nosologies. *J Abnorm Psychol.* 2017;126(4):454–477. doi:10.1037/abn0000258
77. Anticevic A, Cole MW, Murray JD, Corlett PR, Wang XJ, Krystal JH. The role of default network deactivation in cognition and disease. *Trends Cogn Sci.* 2012;16(12):584–592. doi:10.1016/j.tics.2012.10.008
78. Kaminski A, You X, Flaharty K, *et al.* Cingulate-prefrontal connectivity during dynamic cognitive control mediates association between *p* factor and adaptive functioning in a transdiagnostic pediatric sample. *Biol Psychiatry Cogn Neurosci Neuroimaging.* 2023;8(2):189–199. doi:10.1016/j.bpsc.2022.07.003
79. Segal A, Parkes L, Aquino K, *et al.* Regional, circuit and network heterogeneity of brain abnormalities in psychiatric disorders. *Nat Neurosci.* 2023;26(9):1613–1629. doi:10.1038/s41593-023-01404-6